this for conventional CT scanners and results illustrated the fall in dose with patient size increase for constant scanner output. The CBCT system geometry differs significantly from conventional CT scanners. E.g. imaging beams are divergent in the longitudinal direction; beams are offset when using medium/large FOV, not exposing the entire patient in every projection; and partial rotation imaging protocols are used. Therefore it is of interest to test if the relationship between phantom size and dose matches that of fan beam CT.

Materials and Methods: An Elekta XVI CBCT system has been simulated using GATE, the Geant4 Application for Tomographic Emission. Validation measurements in water, of the CBCT beam profile and percentage depth dose, and dose measurements in cylindrical CTDI phantoms all show good agreement with simulated equivalents.

CTDI phantoms with diameters ranging from 12 to 48cm were simulated and used to calculate weighted cone beam dose indices ($CBDI_w$) [2]. Small and medium FOV collimators were used in the simulations, with 120kV x-ray beam and bow-tie filter.

Results: CBCT imaging dose falls with increasing patient size (Fig. 1). Results were comparable to those presented in [1], with fall in dose with size being slightly steeper than the average reported for fan beam CT at 120kV.

$CBDI_w$ uses 1/3 central + 2/3 peripheral dose to estimate average dose within the FOV. The CBCT simulation has been used to test this approximation for CBCT. Average dose received by corresponding voxels of the phantoms is within 2% of the $CBDI_w$ values for phantoms up to 32cm in diameter.

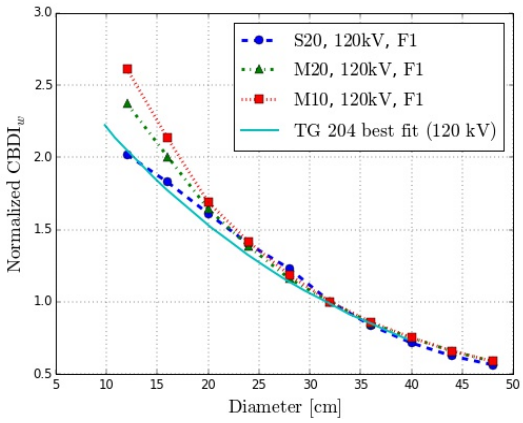

Conclusions: Monte Carlo simulations showed that CBCT imaging dose falls with patient size, in line with expectations from fan beam CT. These results can be used to predict doses and define optimised imaging protocols for large and small patients.

[1] https://www.aapm.org/pubs/reports/RPT_204.pdf
[2] http://dx.doi.org/10.1259/bjr/80446730

PO-0974

Evaluation of quality metrics for CDRAD radiographical images

R. Redondo[1], G. Bueno[1]
[1]*Universidad de Castilla La Mancha, Visilab, Ciudad Real, Spain*

Purpose/Objective: The radiography technology has evolved from common screen-film machinery to photostimulated luminescence (computerized radiography), charge coupled devices (CCD), photoconduction or recently flat panel detectors. One common trade-off is the balance between radiation vs. diagnosis, minimizing the irradiation dose without impairing image contrast and therefore pathology detection rates. However the calibration of these equipment is tedious and sophisticated. Nowadays medical phantoms such as CDRAD(c) have become an standard. However the visual evaluation of phantom images is again a tedious task and not always precise due to technical conditions and observer conditions. Besides the CDRAD Analyzer, in this study we want to carry out an evaluation of 10 general purpose image quality metrics.

Materials and Methods: CDRAD phantoms (see Fig. 1) are made of an acrylic 8 mm thick in which circular flat-topped holes are drilled progressively in a square region of about 15×15mm2. 66 CDRAD images have been acquired with increasing Entrance Surface Dose (ESD) from 1 to 15 mGy. Objective image quality metrics intend to capture fidelity between a dis- torted image and a reference image. Some purely mathematical full-reference metrics were tested together with other metrics more complex in terms of computer vision like Mean Structural Similarity Measure, Visual Signal-to-Noise ration, Information Fidelity Criterion, Visual Information Fidelity or Singular Value Decomposition and Visual Difference Predictor.

The psychophysical experiments followed the procedure Single Stimulus Continuous Quality Evaluation (SSCQE) in ITU-R BT.500-11, without exceeding time. The number of qualified observers were 10.

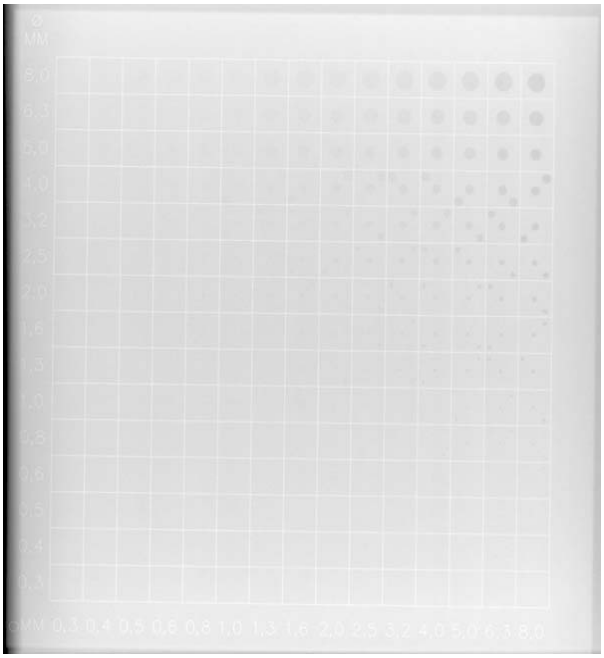

Results: The Cross-Correlation (CC) and Mean Root Square Error (RMSE) of Mean Opinion Scores (MOS) are presented in Table. 1. The CDRAD Analyzer by Artinis makes use of a priori knowledge and although it is not general purpose, that

optimization delivers the highest correlation, above 0.9 and the lowest error 0.18.

METRIC	CC. Spearman	CC. Pearson	RMSE
CDRAD Analyzer	**0.94**	**0.96**	**0.18**
VDP	**0.71**	0.78	0.43
IFC	**0.80**	0.81	0.36
MSSIM	0.35	0.32	0.66
SVD	-0.08	-0.12	0.68
UQI	**0.82**	0.85	**0.36**
VIF	**0.91**	**0.93**	**0.23**
RMSE	-0.43	-0.42	0.64
CrossCorr	0.05	-0.01	0.69
L2-norm	-0.43	-0.43	0.64
Pearson-Coeff	0.58	0.54	0.56

Table 1: Performance of image quality metrics (IQI) against Mean Opinion Score (MOS).

Conclusions: In the present study a bench of 10 image quality metrics have been tested. The study revealed that at least one VIF delivered high correlated scores with pshycophysical observations, and another two UQI and IFC delivered noticeable results. Although their performance is bellow the commercial software delivered by Artinis CDRAD Analyzer, an interesting feature of these metrics is that they do not require any previous knowledge of the image. In that sense they could not require any type of pre-registration process or equalization and could be employed more generally for other medical images like CDMAM, ETR1, TOR,... etc. Future research works will evaluate these metrics for different medical images types.

PO-0975

Quantitative assessment of 3D geometric accuracy of a 1.5T wide-bore MR-simulator: a phantom study

M.W.K. Law[1], J. Yuan[1], G.G. Lo[2], A.Y. Ding[1], O.L. Wong[1], K.F. Cheng[3], K.T. Chan[3], K.Y. Cheung[1], S.K. Yu[1]

[1]Hong Kong Sanatorium & Hospital, Medical Physics and Research Department, Happy Valley, Hong Kong (SAR) China

[2]Hong Kong Sanatorium & Hospital, Department of Diagnostic & Interventional Radiology, Happy Valley, Hong Kong (SAR) China

[3]Hong Kong Sanatorium & Hospital, Department of Radiotherapy, Happy Valley, Hong Kong (SAR) China

Purpose/Objective: To quantitatively assess 3D geometric distortion of MR images acquired on a 1.5T wide bore (70cm diameter) MR-simulator (Optima MR450w, GEHealthcare, Milwaukee, WI), using a large customized geometry accuracy phantom consistent with NEMA MS 12-2010 standard.

Materials and Methods: A large phantom (size LxWxH in cm: 55x55x37.5) was constructed by following NEMA MS 12-2010 standard, made of polyurethane foam (invisible in MR and CT) layers embedded with spherical paintball markers (6mm diameter, visible in MR and CT) arranged on a 3D grid matrix (isotropic interval of 25mm). (Figs a, b). A reference phantom image was acquired on a CT-sim scanner (Lightspeed RT16, GEHealthcare, Milwaukee, WI). 3D fast spoiled gradient echo sequence was used in MR acquisition TR/TE=5.8/2.5ms, FOV=500mm, isotropic voxel size=1.3mm, Flip angle=60°, NEX=4, receiver bandwidth =62.5kHz, with geometric correction). Axial, sagittal and coronal images were individually acquired within a single scan. A Matlab (Mathworks, Natick, MA) script was developed to 1) automatically locate all markers in both MR and CT images; 2) establish correspondence between markers in MR and CT images; 3) compute positional deviation of markers to quantify geometric distortion. Absolute marker deviation was calculated as the 3D distance between the marker position in MR image and its corresponding position in CT image.

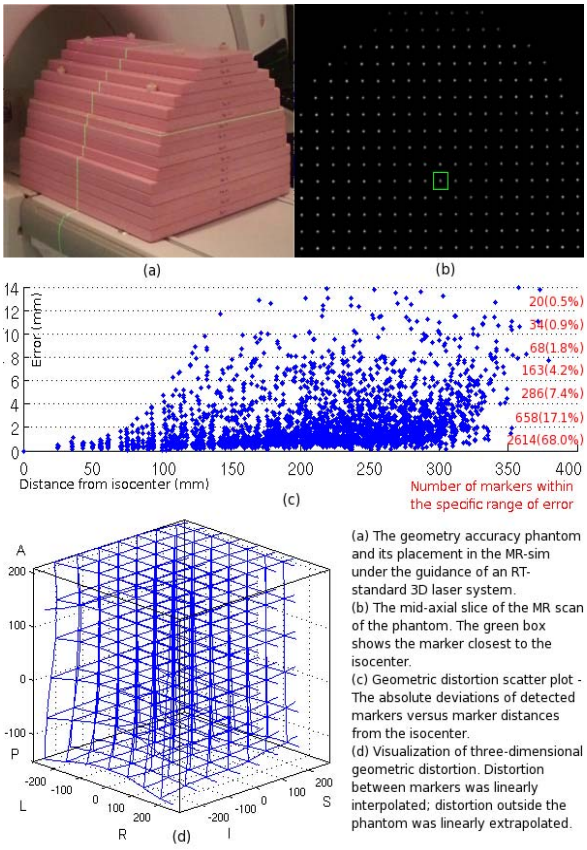

(a) The geometry accuracy phantom and its placement in the MR-sim under the guidance of an RT-standard 3D laser system.
(b) The mid-axial slice of the MR scan of the phantom. The green box shows the marker closest to the isocenter.
(c) Geometric distortion scatter plot - The absolute deviations of detected markers versus marker distances from the isocenter.
(d) Visualization of three-dimensional geometric distortion. Distortion between markers was linearly interpolated; distortion outside the phantom was linearly extrapolated.

Results:

Diameter Sphere Volume, DSV (mm)	Aboslute deviations of markers (mm)					
	Axial scan		Coronal scan		Sagittal scan	
	Average	Maximum	Average	Maximum	Average	Maximum
600	2.2585	22.3508	**1.9314**	**16.7264**	2.2933	20.4956
500	2.0089	22.3508	**1.7229**	**16.7264**	1.9768	20.4956
400	1.5916	14.9561	1.4215	**12.9021**	**1.3699**	15.1297
300	1.1079	**9.1764**	1.1946	11.7039	**0.8952**	9.2808
250	0.7375	**3.7920**	1.0262	8.9010	**0.5875**	4.4360
200	0.6061	2.4906	0.6965	3.7193	**0.4113**	**1.9393**
150	0.5513	1.7085	0.5476	1.8184	**0.3394**	**1.1942**
100	0.4260	1.2429	0.4395	1.0913	**0.2572**	**0.9017**

Table 1. The relation of absolute deviations of detected markers and the markers within a certain distance from the isocenter in CT. The lowest average and maximum values of each distance among three acquisitions were bolded.

The average and maximum deviations of markers are listed in Table.1. The sagittal acquisition achieved a <1mm maximum deviation for 100mm DSV, comparable to the image distortion requirement of a CT simulator (AAPM TG-66 Section III-D-4) for treatment planning. The sagittal acquisition outperformed others upto 200mm DSV, while coronal acquisition showed the lowest deviations when DSV≥500mm. The average deviations were smaller or close to 1mm and 2mm within a DSV of 250mm, and 500mm respectively. Considering low marker deviations, coronal acquisition was